The Heterogeneous Phase Behavior of the Helium-Nitrogen System

N. C. RODEWALD, J. A. DAVIS, and FRED KURATA

University of Kansas, Lawrence, Kansas

This paper deals with the phase behavior of the helium-nitrogen system from 77° to 50°K. The phase behavior investigated was the lower region of the liquid-vapor area, the S-L-V locus, the S-L, and S-V areas. To establish the reliability of the experimental technique, an isotherm at 77°K. was compared with reported data.

In addition to providing more extensive phase-behavior data on the helium-nitrogen system, the data will contribute to the meager understanding of intermolecular forces and of phase behavior in general. Further, the data will allow the testing of thermodynamic relationships.

The data will also be useful in the removal of crude helium from natural gas and its subsequent purification. There are currently under construction several separation plants in which crude helium will be separated from natural gas. The crude helium will be purchased by the U.S. Bureau of Mines who will store the crude gas and purify it to meet future demands.

In order to establish the published data on this system, a literature survey was made. The important aspects of each published investigation are summarized in Table 1, which lists the various investigators in chronological order. Comparison of the data of these eight publications reveals that a variety of experimental methods and gas analysis techniques were used; a large number of isotherms have been investigated from the normal boiling point of nitrogen, 77°K., to its critical temperature, 126°K.; the upper pressure limit of most investigations is 2,000 to 3,000 lb./sq. in. abs.; data below 77°K. are meager; and surprisingly large differences, which range from a maximum of 25 to a minimum of about 5%, exist in the data.

N. C. Rodewald is with the Continental Oil Company, Ponca City, Oklahoma; J. A. Davis is with the Marathon Oil Company, Littleton, Colorado.

THE EXPERIMENTAL EQUIPMENT

The experimental equipment consisted of three major parts, the controllable low-temperature environment, the glass equilibrium cell, and sample make-up and supply.

The Cryostat

The design and fabrication of a low-temperature environment for operation below liquid-nitrogen temperature is discussed elsewhere (*4, 5*). The purpose of this cryostat was to provide accurate temperature measurement and control for the glass equilibrium cell. Temperature measurement was made with a platinum resistance thermometer used in conjunction with a bridge and an electronic null detector. Estimated accuracy of the calibration technique for the temperature range of this study was ± 0.03°K. to ± 0.07°K.

Bath temperature was controlled to within 0.02°K. with a modified controller.

Glass Equilibrium Cells

The Pyrex glass equilibrium cells used to make the liquid-vapor measurements had volumes of 3.5 to 5 cc. and could safely withstand pressures to 1,000 lb./sq. in. abs. Volume

TABLE 1. PUBLISHED HELIUM-NITROGEN PHASE BEHAVIOR DATA

Investigator	Year	Pressure range, lb./sq. in. abs.	Temperatures of *P-x* diagrams, °K.	Experimental method	Gas analysis
Porter (*18*)*	1929	Unknown	77.6 to 123.1	Unknown	Unknown
Fedoritenko and Ruhemann (*7*)	1937	75 to 2,200	64, 78, 90, 108	Flowing-condensation, static	Heat conductivity
		20, 4 atm.†	64 to 116		
Gonikberg and Fastowsky (*8*)	1940	220 to 4,200	78, 90.1, 109	Circulation method	Gas density
Jenkins and Hillery (*3*)**		400 atm.	78.0	Unknown	Unknown
Kharakhorin (*11*)	1940	60 to 3,200	68, 77.3, 90.1, 107, 111.5	Circulation method	Heat conductivity
Swenker and Dokoupil (*17*)	1955	15, 10, 5 atm.†	65 to 35	Flow method	Freezing
Buzyna (*1, 2*)	1962	170 to 1,000	77.2, 92.8, 112.1, 118.5, 122.8	Dew and bubble point, static	Mass spectrometer
DeVaney, Dalton, Meeks (*6*)	1963	200 to 2,000	76.5, 80, 85, 95, 100, 105, 110, 115, 120	Static	Gas chromatograph
McKinley (*19*)††		0 to 120	68.0	Unknown	Unknown

* Data presented in the form of a temperature vs. mole percent helium in liquid per atmospheric partial pressure helium plot.
† *T-x* diagram.
** Unpublished data at Linde, only liquid-vapor concentrations at these conditions.
†† Unpublished data at Air Products and Chemicals, Inc.

TABLE 2. COMPOSITION OF MIXTURES STUDIED

Mixture	Composition, mole % helium
1	0.100
2	0.500
3	70.39
4	90.41
5	96.09
6	6.19
7	55.4
8	90.52
9	3.17
10	98.30
11	99.00
12	99.500

The composition uncertainty for mixtures 1, 2, 10, 11, and 12; mixtures 3, 4, 5, and 7; and mixtures 6, 8, and 9 are believed to be, respectively, ±3% of the minor component, ±0.1 mole %, and ±0.02 mole %.

percent vs. liquid height measurements were made with a cathetometer to a precision of about 0.2 volume %. Imperfections in the glass slits of the Dewars caused this uncertainty.

Heavy walled cells having a bore of about 0.1 in. (1-cc. volume) were safely used to 2,000 lb./sq. in. abs. to study S-L and S-L-V behavior.

Cell pressures were read on a bourdon tube gauge to an accuracy of ± 0.5 lb./sq. in. abs.

Sample Make-up and Supply

This unit served as a gas reservoir which maintained the gas mixture to be studied at a constant temperature. It permitted accurate metering of gas to the cell and making up of mixtures of predetermined compositions. The latter was especially important for mixtures containing less than 1% of the minor component, since common analytical techniques are usually no better than ± 0.02 mole %. However, all volumetric compositions were checked by either mass spectrometer and/or gas density measurements. Table 2 gives the mixture composition selected as being the most reliable.

The maximum expected volumetric error, which was primarily caused by the lack of sensitivity of a pressure gauge, was about ± 0.5%.

THE EXPERIMENTAL PROCEDURE

No attempt will be made to discuss the operation of the equipment, since this has been done elsewhere (*4, 5*). Emphasis will be placed on the techniques for measuring the phase behavior.

Liquid-Vapor Behavior

Liquid-vapor behavior was established by the use of the dew- and bubble-point method. Since the difference between dew and bubble pressures for most mixtures is of the order of thousands of pounds, dew pressures were established for mixtures ranging from 55 to 96 mole % helium, and bubble pressures were fixed for mixtures containing less than 1 mole % helium. Dew pressures were determined graphically from plots of the quantity metered to the cell vs. cell pressure. At the dew point, there is a break in the curve. The process is represented on a typical P-T diagram by the line starting at A on Figure 1. Bubble-point measurements are merely a continuation of this line.

In addition, another method for the calculation of liquid and vapor compositions together with saturated volumetric properties was developed and successfully used (*14, 15*). The data for these calculations require only quantities measured in the determination of the dew and bubble points. The phase rule specifies that, for an isothermally univariant system, if the pressure is fixed, the intensive properties X, Y, ρ^l, and ρ^g are fixed regardless of the volume percent liquid.

A numerical solution for these variables requires four simultaneous equations. Since it is possible to write two equations from material balances on nitrogen and helium at each volume

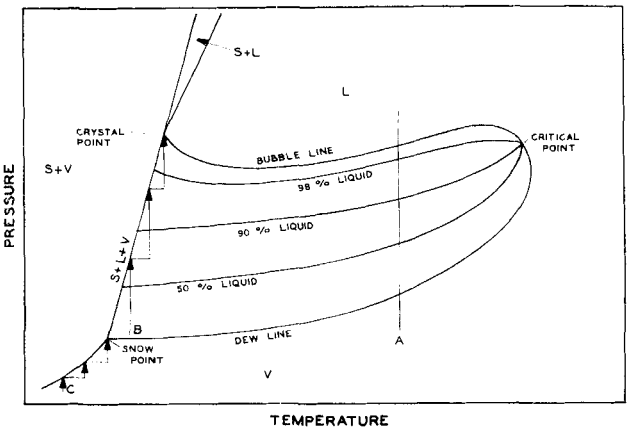

Fig. 1. Phase diagram of a helium-nitrogen mixture.

percent liquid, two independent runs are required. The quantities which must be measured are the amount of known composition gas metered to the cell and the volume percent liquid at cell conditions. The equations are as follows:

$$Y = \frac{X_f n_1 V_2^l - Y_f n_2 V_1^l}{n_1 V_2^l - n_2 V_1^l} \tag{1}$$

$$X = \frac{X_f n_1 V_2^g - Y_f n_2 V_1^g}{n_1 V_2^g - n_2 V_1^g} \tag{2}$$

$$\rho^l = \frac{n_2 V_1^g - n_1 V_2^g}{(V_1^g - V_2^g) V_c} \tag{3}$$

$$\rho^g = \frac{n_1 V_2^l - n_2 V_1^l}{(V_2^l - V_1^l) V_c} \tag{4}$$

In applying the preceding four equations, it is desirable to make the difference in the numerators and denominators as large as possible. This can be done by making one run near the bubble point and the other run near the dew point. In the limit, these equations go to the dew and bubble points.

Procedure for Determining S-L-V Locus

Data defining this univariant line were obtained by starting with about 10 volume % liquid nitrogen in the cell and adding helium gas as necessary to establish the initial pressure in the cell. The bath temperature was slowly lowered, while the contents of the cell were vigorously agitated to ensure equilibrium. The point at which crystals first began to form was visually noted. The bath temperature was slowly increased until all but a very few of the crystals disappeared. This process was repeated until the temperature difference between appearance and disappearance of the crystals was about ± 0.02°C. By alternately injecting pure helium into the cell and raising the bath temperature, it was possible to determine several points on the three-phase locus as indicated by the stepwise function starting at B in Figure 1.

Crystal points similar to those labeled on Figure 1 were obtained by using a procedure identical to the one in the preceding paragraph, with the exception that the gas injected into the cell was the gas mixture under study. At the crystal point,

TABLE 3. EXPERIMENTAL P-T DATA FOR THE S-L-V LOCUS

Pressure, lb./sq. in. abs.	Temperature, °K.
1.85	63.15
260	63.53
560	63.90
760	64.09
898	64.32
1,221	64.75
1,610	65.17
2,016	65.67

TABLE 4. DEW-POINT MEASUREMENTS

Composition, mole % helium	Temperature, °K.	Dew pressure, lb./sq. in. abs.
55.4	77.2	36.3
55.4	69.3	12
55.4	64.9	6.5
70.4	77.1	55.3
70.4	69.1	28.5
70.4	64.1	26
90.4	77.1	162
90.4	69.1	67.2
90.4	69.1	66
90.4	65.0	60
96.1	77.2	480
96.1	69.1	175*
96.1	65.0	76*
96.1	63.3	63.2*

* No sharp break.

there is only an infinitesimal amount of vapor and solid in equilibrium, with the cell full of liquid.

Procedure for Determining the S-V Data

The technique used here is similar to that discussed in the preceding two paragraphs. The step-by-step P-T path followed is indicated by the line starting at point C in Figure 1.

THE EXPERIMENTAL RESULTS

The experimental outline followed in this work was to determine first the lower limit of the vapor-liquid region, which is the S-L-V locus. The upper temperature limit of the L-V region was selected as 77°K. Within this temperature limit, the L-V behavior was established for isotherms of 77.2°, 69.3°, and 64.9°K. by using the dew- and bubble-point method along with the developed calculational method. Saturated liquid and vapor density data were obtained concurrently with the V-L phase data. In addition, S-V behavior of several mixtures prepared for dew-point measurements and three other mixtures was studied. Crystal points were established for the bubble mixtures.

The Pressure Temperature Relationship of the S-L-V Locus

The original data for pressure-temperature relationship of the S-L-V locus are plotted in Figure 2, and some are given in Table 3. The dashed line is the melting curve for

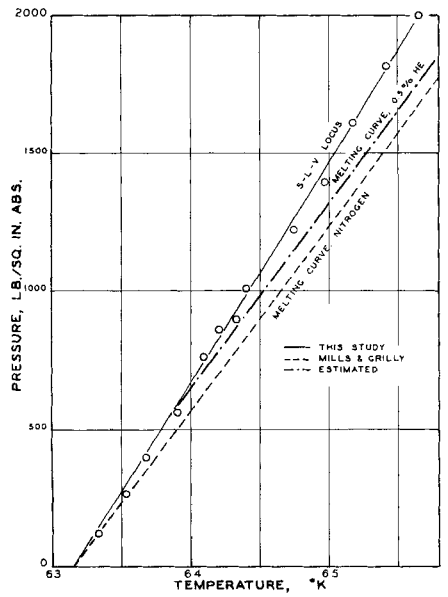

Fig. 2. Pressure-temperature relationship of the solid-liquid vapor locus.

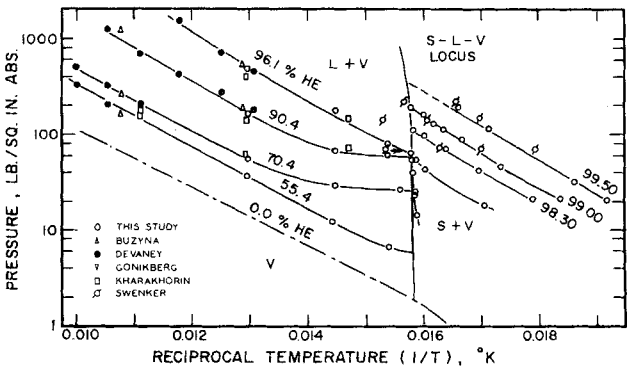

Fig. 3. Semi-log P-T plot for dew mixtures.

nitrogen (9). The deviation of the data from the smooth curve is ± 0.03°K. The slope of the S-L-V line is such that a temperature change of 0.01°K. corresponds to 3.97 lb./sq. in.

Since helium gas at the S-L-V locus is far above its critical temperature and only slightly soluble in liquid nitrogen, the P-T curve should closely approximate the melting curve of pure nitrogen, with the helium in solution slightly depressing the freezing point of nitrogen. At higher pressures, the freezing point depression increases owing to higher helium solubility.

Dew-Point Measurements

To establish vapor compositions at low pressures, dew-point measurements for mixtures containing 55.4, 70.4, 90.4, and 96.1 mole % helium were made. The actual dew points (Table 4) were determined graphically from plots of quantity of gas metered to the cell as a function of cell pressure. There was a sharp break in the curve for the 55.4 and 70.4 mole % helium mixtures. However, as the amount of nitrogen in the mixture decreased, the break in the curve became less discernible and was almost nonexistent for the 96.1 mole % helium mixture. Thus, it was impractical to use this approach for mixtures containing more than 96 mole % helium. The uncertainty in the dew pressures determined graphically is ± 1 lb./sq. in. or ± 1% (whichever is larger) for the 55.4 and 70.4 mole % helium mixtures, ± 5% for the 90.4 mole % helium mixture, and ± 10% for the 96.1% helium mixtures.

Solid-Vapor Behavior

The solid-vapor behavior of three dew-point mixtures and three other mixtures was studied. These data are

TABLE 5. SUMMARY OF THE S-V BEHAVIOR

Composition, mole % helium	Temperature, °K.	Dew pressure, lb./sq. in. abs.
70.4	63.78	14.0
90.52	63.14	23.6
90.52	63.20	40.3
90.52	63.20	54.3
96.1	58.65	17.7
96.1	63.05	53.7
98.30	55.99	20.8
98.30	61.09	71.8
98.30	63.32*	115.4
99.00	54.32	20.8
99.00	60.03	91.2
99.00	61.80	132.2
99.00	63.28	193.3
99.500	53.88	34.5
99.500	60.30	197.6

* Possibly on S-L-V locus.

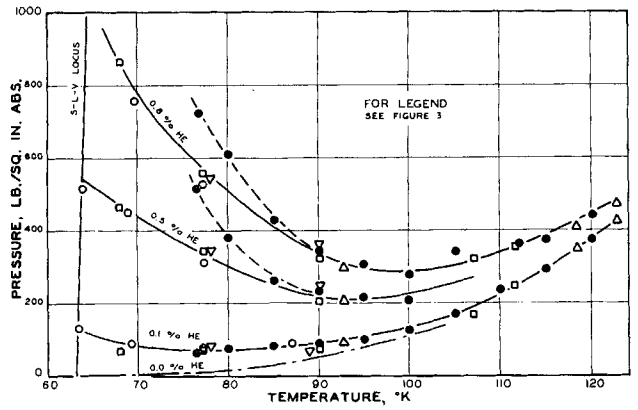

Fig. 4. P-T relationship of the bubble mixtures.

summarized completely in Figure 3 and partially in Table 5. For all mixtures except the 99.500 mole % helium mixture, the difference between appearance and disappearance of the solid was within ± 0.02° to ± 0.05°K. The amount of solid freezing from the 99.500 mole % helium mixture was very minute; consequently, the exact snow points could be defined to only ± 0.5°K.

The pressure-temperature relationships for the dew lines and the S-V lines of the gas mixtures are shown in Figure 3. Since pure nitrogen exhibits nearly a straight line on the semilogarithmic plot of this type, the dew lines should exhibit similar behavior. As shown, the curvature becomes significant only near the S-L-V locus. The S-V and dew lines for the same mixture must terminate at the same point on the S-L-V locus. The snow points for the dew and S-V mixtures are summarized in Table 6.

The P-T data of other investigators for the composition parameters under consideration are also shown in Figure 3. The data of the various investigators scatter about a smooth curve with no consistent deviation. As a result, the tie in between the low temperature data of this study and Swenker (*17*) with those other investigators at higher temperatures is quite satisfactory. However, Swenker did present several S-V data points in the L-V region.

An exploratory run was made to observe visually the phases present tin the temperature range from 50° to 10°K. up to 1,000 lb./sq. in. abs. Initially, 5 to 10% of the cell volume was filled with liquid nitrogen. Then the system was pressurized with helium gas, and the bath temperature was lowered to the first isotherm. The pressure was varied in 100 lb./sq. in. increments; then the bath temperature was lowered to the next isotherm and the process repeated. Within these temperature and pressure limits, only solid and vapor phases were observed. The composition of the vapor phase in equilibrium with solid nitrogen was not determined.

Bubble-Point Measurements

Bubble-point measurements were made on two mixtures, 0.100 and 0.500 mole % helium. Because of the sizeable increase of pressure near complete condensation, a plot of reciprocal pressure vs. volume percent [recommended by Mullhaupt and Di Paolo (*13*)] was used to extrapolate to 100%. In most cases, this plot was essentially a straight line. Still the uncertainty estimated for the bubble-point pressure in Table 7 is ± 10%.

Table 6. Three-Phase Vapor Composition

Composition, mole % helium	Pressure, lb./sq. in. abs.
55.4	5.8
70.4	26.0
90.5	58.0
96.1	63.0
98.30	115.0
99.00	199.0
99.500	350*

* Extrapolated.

Table 7. Experimental Bubble Points

Composition, mole % helium	Temperature, °K.	Pressure, lb./sq. in. abs.
0.100	87.1	92
0.100	77.2	78
0.100	69.3	94
0.500	77.2	312
0.500	69.3	450

The experimental crystal point for Mixtures I and II were, respectively, 135 and 520 lb./sq. in. abs. Since it was exceedingly difficult to define the exact crystal points at 100 volume % liquid, the uncertainty here is about ± 10% of the pressure.

Figure 4 shows the P-T relationship for the two bubble-point mixtures and a third mixture from 120°K. to the S-L-V locus. It should be noted that the bubble pressure goes through a minimum and increases until the curve intersects with S-L-V locus. This phenomenon has been named *reverse order solubility*. In this plot the data of this study and those of other investigators are shown. In general, the data of this study, Buznya, Kharakhorim, and Gonikberg, scatter about a smooth curve. Below about 85°K., however, DeVaney observed helium to be considerably less soluble than did the other investigators.

The bubble curves intersect the S-L-V locus at the crystal points. The S-L lines for the mixtures lie slightly to the right of the S-L-V locus and terminate at the crystal points as the schematic diagram, Figure 1, shows. Figure 2 shows an estimated melting curve for the 0.500 mole %

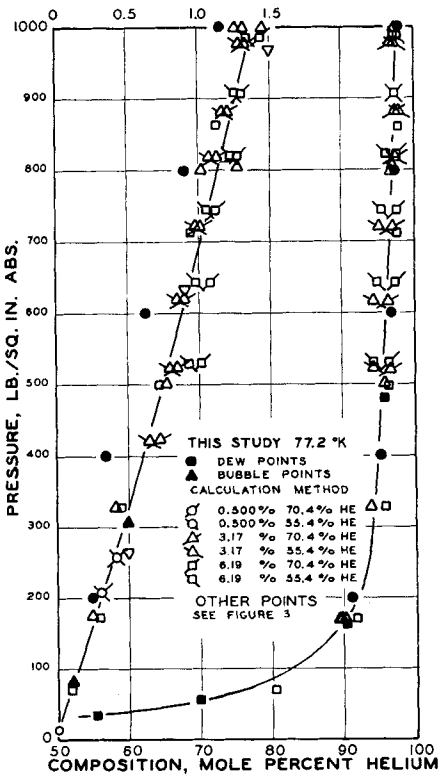

Fig. 5. Pressure-composition diagram.

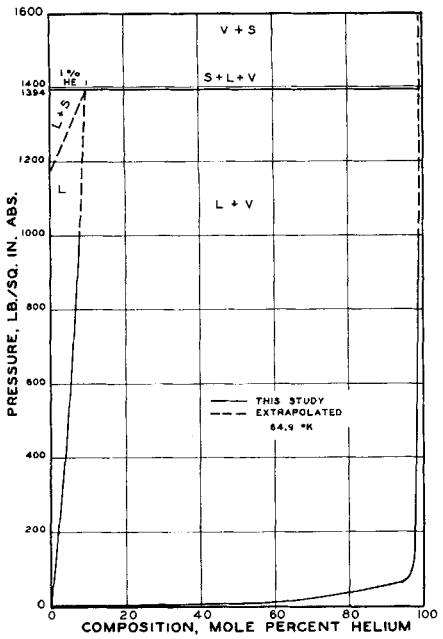

Fig. 6. Pressure-composition diagram, 64.9°K.

helium mixture and indicates that it lies in the narrow P-T area between the melting curve of nitrogen and the S-L-V locus. Because of its proximity to the S-L-V locus, it has not been included in Figure 4.

Calculated Liquid-Vapor Behavior

Since the usefulness of the dew- and bubble-point method for determining the *X-Y* data of slightly soluble gases in liquids is limited, the derived calculation method was used to determine the majority of the data. In applying Equations (1) through (4), a combination of five mixtures was used. Two mixtures, 55.4 and 70.4 mole % helium, gave low volume percent liquid; three mixtures, 0.500, 3.17, and 6.19 mole % helium, resulted in high volume percent liquid. In order to eliminate any smoothing error on the P-volume percent data of the bubble isotherm, *X-Y* values were calculated for the experimental points on the bubble isotherms. This was necessary because of the very steep rise of pressure near a bubble point. Since two sets of data points are available for the dew isotherm, it was possible to calculate two liquid and two vapor compositions for each bubble point. The results for the 77.2°K. isotherm are summarized in Figure 5. The P-X diagrams for 69.3° and 64.9°K., the pressure-volume percent data, and all the calculated data can be found elsewhere (*14*).

The average deviation of the liquid composition points from a smooth curve through the data at 77.2°, 69.3°, and 64.9°K. is 0.05 mole % helium for each isotherm. The maximum deviation is 0.23 mole % helium. For the vapor-phase composition at 77.3°, 69.3°, and 64.9°K., the average deviation is 0.08, 0.08, and 0.04 mole % helium, respectively. Since the dew-point determinations were considered more reliable at low pressure than calculated values, only dew-point data are shown in the lower range. Smoothed *X-Y* data are presented in Table 8.

The effects of measurement errors of the independent variables in Equations (1) and (2) on the calculated *X-Y* values were estimated from the total differential equation (*15*). The estimated maximum error was about twice the average deviation and four times the average deviations in Equations (1) and (2), respectively. The error analysis also showed that measurement errors in volume percent liquid and quantity metered to the cell contributed most to the *X* and *Y* uncertainty. The *X-Y* data were also tested for thermodynamic consistency and correlativity (*14*).

Table 8. Smoothed *X*, *Y*, ρ^1, Z^g Data

	X	*Y*	ρ^1	Z^g
	Temperature = 77.2°K.			
200	0.31	92.0	0.02910	1.00
400	0.62	95.5	0.02930	1.039
600	0.91	96.8	0.02945	1.070
800	1.175	97.5	0.02959	1.098
1000	1.38	97.9	0.02971	1.124
	Temperature = 69.3°K.			
200	0.24	97.3	0.03017	1.029
400	0.46	98.0	0.03026	1.064
600	0.66	98.3	0.03034	1.094
800	0.83	98.5	0.03042	1.121
1000	0.95	98.8	0.03049	1.146
	Temperature = 64.9°K.			
200	0.19	97.7	0.03083	1.024
400	0.365	98.1	0.03091	1.055
600	0.51	98.5	0.03099	1.084
800	0.63	98.8	0.03108	1.114
1000	0.73	99.2	0.03116	1.146

Note: Units for X and Y, mole % helium.
Units for ρ^1, g. mole/cc.

Figure 6 shows the P-X relationship at 64.9°K. replotted and extended to slightly higher pressure. This was done to illustrate the termination of L-V area at the three-phase locus. The three-phase pressure can be read directly from Figure 2 to be 1,390 lb./sq. in. abs. This diagram also fixes the melting pressure of pure nitrogen and a 0.500 mole % helium mixture at 1,175 and about 1,270 lb./sq. in. abs., respectively. These two melting pressures were used to establish the boundary of the narrow L-S region which starts at the melting point of nitrogen and terminates at the S-L-V locus. The phases present in the various areas are shown in this diagram.

Fedoritenko (7) indicated in the graphical presentation of his P-X curves that he experimentally measured L-V behavior at 64°K. to 140 atm. (2,060 lb./sq. in. abs). Since the S-L-V locus slopes forward from the triple point of nitrogen, the validity of these data is questionable. He measured L-V data in a region where only S-V can exist.

Figure 7 shows the T-X curves for the liquid phase at 200, 500, 1,000, and 2,000 lb./sq. in. abs. Since the curves for higher pressures lie close together, only the vapor curve for the 200 lb./sq. in. abs. isobar is shown. As shown, the isobaric L-V areas terminate at the S-L-V locus. Because of the forward slope of the S-L-V locus, the iso-

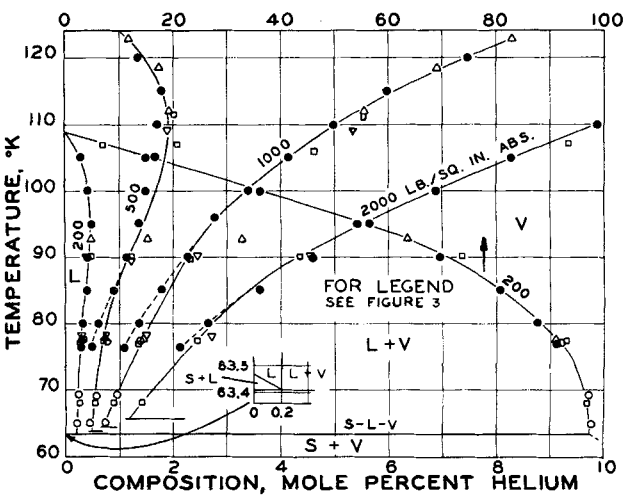

Fig. 7. Isobaric temperature-composition plot.

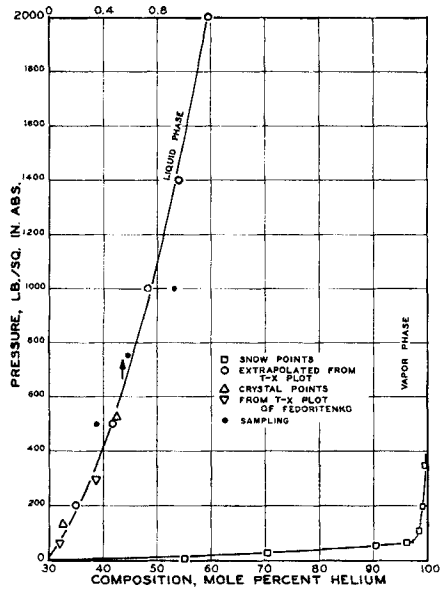

Fig. 8. Three phase vapor-liquid composition.

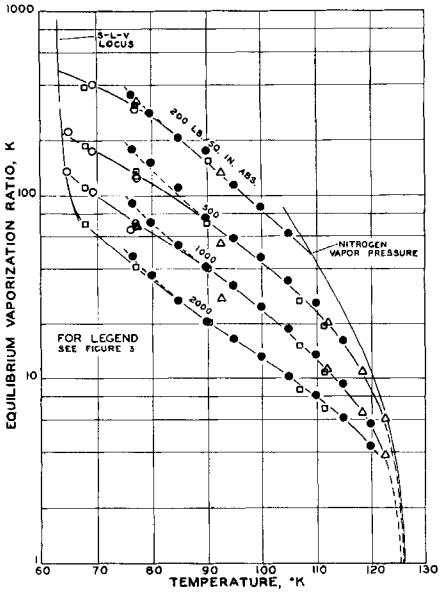

Fig. 9. Isobaric equilibrium vaporization ratio for helium.

bars at higher pressures terminate at higher temperatures.

In order to show plainly the L-S behavior of the 200 lb./sq. in. abs. isobar, an insert has been made. With reference to Figure 2, the temperature limits of this area can be fixed by noting the three-phase and nitrogen melting temperatures at 200 lb./sq. in. abs. to be 63.41° and 63.46°K., respectively. The phases present in the various areas have been indicated. Both the 200 and 500 lb./sq. in. abs. isobars exhibit the reverse order solubility phenomenon, that is the decrease of helium solubility in the liquid phase with decreasing temperature. Fedoritenko, Buzyna, and DeVaney have thoroughly discussed this phenomenon.

Figure 7 also gives a thorough comparison of the helium concentration in the liquid phase. The data of the various investigators define the 200 lb./sq. in. abs. isobar well; however, below 85°K. and from 400 to 2000 lb./sq. in. abs., DeVaney's data deviate significantly from the data of other investigators; and as DeVaney pointed out, Buzyna's data at 92.8°K. above 400 lb./sq. in. abs. show a wide discrepancy from the smooth curve.

It is obvious from Figure 7 that the T-X isobars for liquid can be extrapolated accurately to the three-phase locus to give the limiting composition. Kharakhorin's data were relied upon above 1,000 lb./sq. in. abs. for the liquid phase. As shown in Figure 7, the length of the extrapolation decreases as the pressure increases from 200 to 2,000 lbs./sq. in. abs. Table 9 summarizes the results for the extrapolated isobar. The uncertainty of the extrapolated liquid composition is ± 0.05 mole % helium.

Table 9. Liquid Composition Along the S-L-V Locus

Pressure, lb./sq. in. abs.	X, mole % helium
200	0.20
500	0.47
500*	0.36
750*	0.59
1,000*	0.93
1,000	0.73
1,400	0.96
2,000	1.17
58.9 (4 atm.)†	0.08
294 (20 atm.)†	0.35

* Sampling data.
† Extrapolated from T-X plots of Fedoritenko.

Fedoritenko determined T-X diagrams at two pressures, 4 and 20 atm, by direct experiment and presented these results in graphical form with an expanded scale to bring out the slope of the liquid branch. The liquid branches were extrapolated to the S-L-V locus, and the results are presented in Table 9.

Table 9 also includes several liquid points obtained by sampling and mass spectrometer analysis.

Snow points, crystal points, and three-phase liquid points are graphically summarized in Figure 8.

Equilibrium vaporization ratios for helium were calculated for the same isobars as the T-X curves and are shown in Figure 9. The lower temperature boundary for the helium K values is the S-L-V locus, while the upper boundary is the vapor pressure of nitrogen or the critical temperature.

Although the liquid compositions for the 200 and 500 lb./sq. in. abs. isobars go through a maximum, the K values do not, because the increase in helium vapor composition with decreasing temperature is sufficient to obscure the smooth change of liquid composition near the maximum. This phenomenon is undoubtedly the cause for some of the uneven curvature transition from the 200 to 2,000 lb./sq. in. abs. isobars.

Figure 9 offers a convenient way of comparing both liquid and vapor data. The deviation of DeVaney's data from the smooth curve is 17.5, 10.8, and 5.7 % for 76.5°, 80°, and 85°K., respectively. Although the 1,400 lb./sq. in. abs. isobar is not shown, it was used in the calculation of the percent deviation. The deviation of Buzyna's data for the 500 and 1,000 lb./sq. in. abs. isobars at 92.8°K. is, respectively, 13.5 and 24.2%. The remaining data appear to scatter about a smooth curve.

Saturated Volumetric Data

Saturated volumetric data were obtained concurrently with the determination of the liquid-vapor behavior. All of these data were calculated by the method presented earlier and used for the liquid-vapor behavior calculation.

Example calculations are presented elsewhere (*14, 15, 4*); however, all the calculated points are graphically summarized in Figures 10 and 11. Smoothed data are presented in Table 8. Average deviations of the individual liquid density points from the smooth curves are 0.000088, 0.000037, and 0.000071 mole/cc. for 77.2°, 69.3°, and 64.9°K., respectively. For the saturated compressibil-

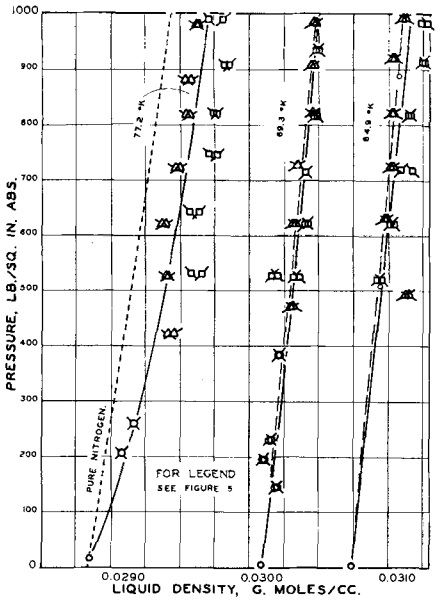

Fig. 10. Saturated liquid density isotherms.

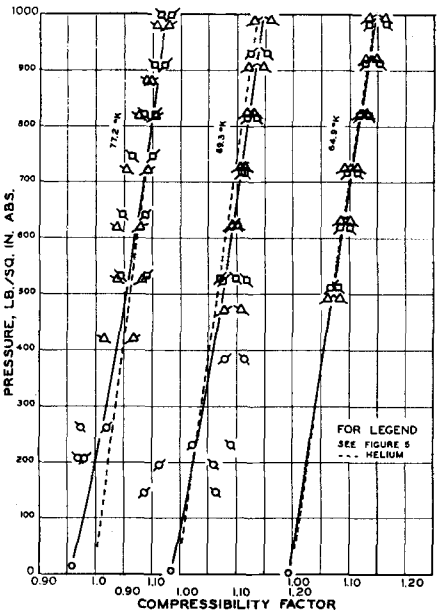

Fig. 11. Saturated compressibility isotherms.

ity factors, the average deviations from the smoothed curves at 77.2°, 69.3°, and 64.9°K. were, respectively, 0.0177, 0.0190, and 0.100 units. From the scatter of the experimental data and the results of an error analysis (*15*), it is believed that the reliability of the data is ± 1% for the liquid density and ± 2% for the compressibility factor.

Included in Figures 10 and 11 are dashed lines which represent the supercooled volumetric properties of nitrogen (*16*) and the superheated properties of helium (*10*). Since the equilibrium phases are nearly pure, it is expected that the saturated volumetric properties of the mixture would approach those of the pure components. For engineering calculations at 77°K. and below, the saturated liquid density and saturated compressibility factors of pure nitrogen, and helium can be used with little error.

ACKNOWLEDGMENT

National Science Foundation Grant 9217 furnished the major portion of the financial support for this work. The financial aid through fellowships by the Marathon Oil Company and Ethyl Corporation is also gratefully acknowledged.

NOTATION

K = equilbrium vaporization ratio for helium
n = quantity of material, g. moles
P = pressure, lb./sq. in. abs.
T = temperature, °K.
V = volume, cc.
X = liquid composition, mole %
Y = vapor composition, mole %
ρ = density, g. moles/cc.

Superscripts

g = gas
l = liquid

Subscripts

c = cell
f = feed
m = mixture
1 = run number for Equations (1) through (4)
2 = run number for Equations (1) through (4)

LITERATURE CITED

1. Buzyna, G., M.S. thesis, Institute of Gas Technology, Chicago, Illinois (1962).
2. ———, R. A. Macriss, and R. T. Ellington, *Chem. Eng. Progr. Symposium Ser. No. 44*, **59**, 101-111 (1963).
3. Cook, G. A., "Argon, Helium, and the Rare Gases," Vol. 2, p. 398, Interscience, New York (1961).
4. Davis, J. A., Ph.D. thesis, The University of Kansas, Lawrence, Kansas (1963).
5. ———, N. C. Rodewald, and F. Kurata, *Ind. Eng. Chem.*, **11**, 36-42 (1963).
6. DeVaney, W. E., B. J. Dalton, and J. C. Meeks, *J. Chem. Eng. Data*, **4**, 473-478 (1963).
7. Fedoritenko, A., and M. Ruhemann, *Tech. Phys. U.S.S.R.*, **4**, 36-43 (1937).
8. Gonikberg, M. G., and W. C. Fastowsky, *Acta Physiochim, U.S.S.R.*, **12**, 67-72 (1940).
9. Johnson, V. J., "A Compendium of the Properties of Materials at Low Temperature (Phase I) Part I Properties of Fluids," National Bureau of Standards, Boulder, Colorado (July, 1960).
10. ———, and R. B. Stewart, Wright Air Development Division, *Tech. Rept. 60-56, Part IV*, National Bureau of Standards, Boulder, Colorado (December, 1961).
11. Kharakhorin, F. F., *Inz. Fiz. Zh. Tekh. Fiz.*, **10**, 1533-1540 (1940).
12. ———, *Inz. Fiz. Zh. Akad. Nauk Belorussk, S.S.R.*, **9**, 24-29 (1959).
13. Mullhaupt, J. T., and F. S. Di Paolo, Paper presented at the ACS Winter Symposium at Washington University in St. Louis, Missouri (December 27, 1960).
14. Rodewald, N. C., Ph.D. thesis, The University of Kansas, Lawrence, Kansas (1963).
15. ———, J. A. Davis, and F. Kurata, *Ind. Eng. Chem.* Fund., 3, No. 1, p. 8 (1964).
16. Strobridge, T. R., *Nat. Bur. Std. Tech. Note 129*, Boulder, Colorado (1962).
17. Swenker, M. D. P., and Z. Dokoupil, *Suppl. Bull., Inst. Intern. Froid, Annexe 1955-1963*, 339. See Dokoupil, Z., *Progr. Low Temp. Phys.*, **3**, 454-480 (1961).
18. U.S. Bureau of Mines, "Open File of Information and Data Relating to the Extraction of Helium from Natural Gas by Low Temperature Processes," Amarillo, Texas (1959).
19. Vance, R. W., "Cryogenic Technology," p. 99, Wiley, New York (1963).

Manuscript received September 23, 1963; revision received March 16, 1964; paper accepted March 17, 1964. Paper presented at A.I.Ch.E. Memphis meeting.